



Syntheses, thermal properties, and phase morphologies of novel benzoxazines functionalized with polyhedral oligomeric silsesquioxane (POSS) nanocomposites

Yuan-Jyh Lee, Shiao-Wei Kuo, Yi-Che Su, Jem-Kun Chen, Cheng-Wei Tu, Feng-Chih Chang*

Institute of Applied Chemistry, National Chiao-Tung University, Hsin-Chu 30050, Taiwan, ROC

Received 4 November 2003; received in revised form 23 April 2004; accepted 27 April 2004

Abstract

We have successfully synthesized a novel benzoxazine ring-containing polyhedral oligomeric silsesquioxane (BZ-POSS) monomer by two routes: (1) hydrosilylation of a vinyl-terminated benzoxazine using the hydro-silane functional group of a polyhedral oligomeric silsesquioxane (H-POSS) and (2) reaction of a primary amine-containing POSS (Amine-POSS) with phenol and formaldehyde. The benzoxazine-containing POSS (BZ-POSS) monomer can be copolymerized with other benzoxazine monomers through ring-opening polymerization under conditions similar to that used for polymerizing pure benzoxazines. Thermal properties of these POSS-containing organic/inorganic polybenzoxazine nanocomposites have been improved over the pure polybenzoxazine analyzed by differential scanning calorimetry (DSC) and thermal gravimetric analysis (TGA). The BZ-POSS monomer is poorly miscible with the benzoxazine monomer and tends to aggregate and forms its own domains, both before and after polymerization. At a higher BZ-POSS content, gross aggregation occurs and results in a lower than expected improvement in the thermal properties.

© 2004 Published by Elsevier Ltd.

Keywords: Polybenzoxazines; polyhedral oligomeric silsesquioxane; Nanocomposites

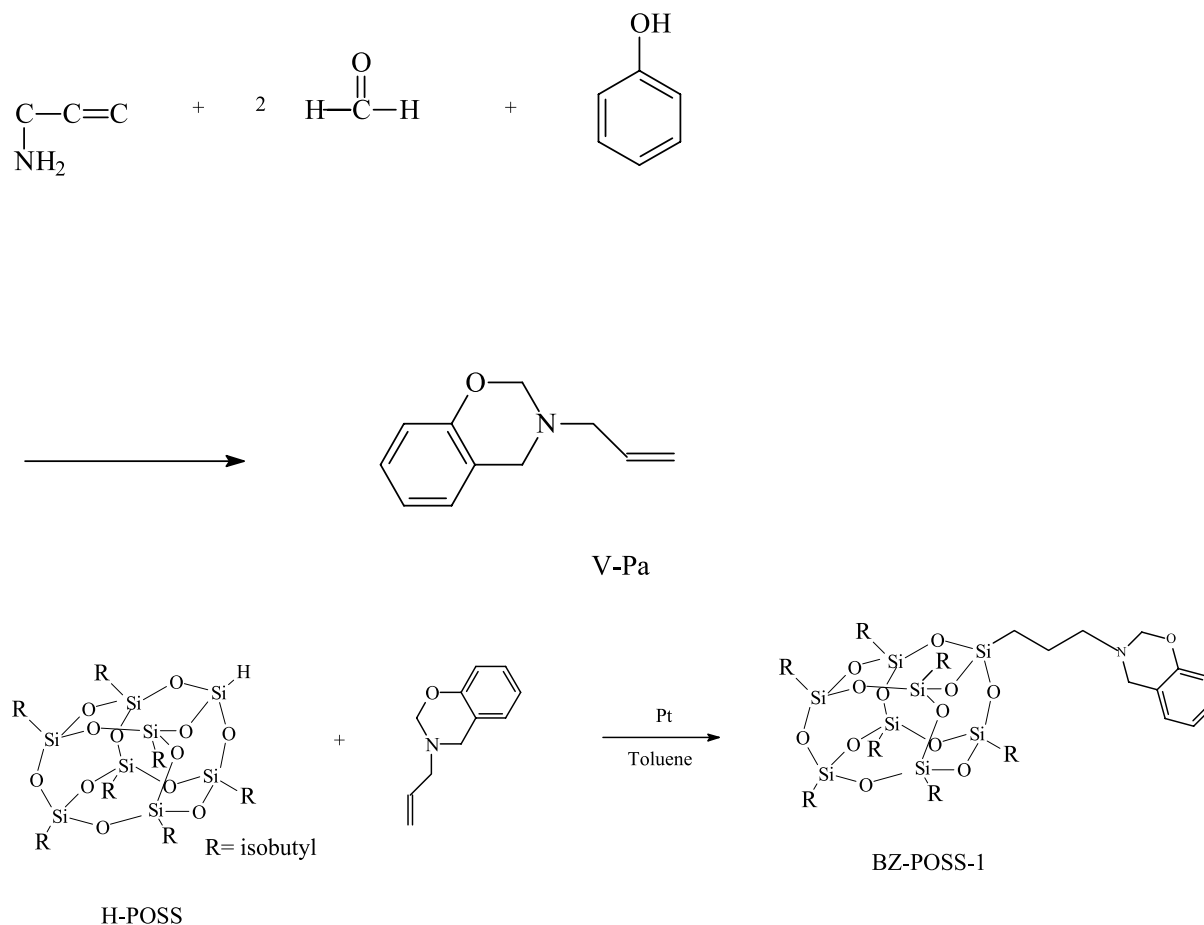
1. Introduction

Benzoxazine monomers are heterocyclic compounds featuring an oxazine ring and are synthesized by the reaction between a primary amine, phenol, and formaldehyde [1–3]. Benzoxazines can be polymerized by ring-opening polymerization in the absence of a catalyst that releases no byproduct. Polybenzoxazines are phenolic-like materials that possess good heat resistance, flame retardant, and dielectric properties [4,5]. Another notable advantage for its application is that raw materials are inexpensive and fabrication is relatively easy. To improve the thermal stability of polybenzoxazines, polymerizable acetylene side groups have been incorporated into the benzoxazine monomers [6–10] that can then be polymerized into three-dimensional networks possessing high stability to thermal oxidation, and resistance to solvents and moisture. Another approach to improve its thermal stability is to blend

with other polymers [11–14] such as poly(vinyl pyrrolidone), poly(imide-siloxane), polyurethane, and epoxy resins into the polybenzoxazine matrices.

Hybrid materials containing both inorganic and organic components are expected to have increased performance capabilities relative to their non-hybrid materials. Due to the nano-length scale involved, nanocomposite materials feature an extensive array of interfacial interactions that can result in salient changes relative to their components' properties [15]. Organic/inorganic hybrid materials prepared by sol–gel methods usually are crosslinked systems whose morphologies and properties often depend on methods by which they are processed. Blends of polybenzoxazine and montmorillonites (clays) have been studied extensively because a small amount of well-dispersed clay layers in the polymer matrix can improve its mechanical and thermal properties. The inorganic layered silicate structure of the clay, however, does not permit it to disperse well in the organic polymer matrix and it is essential to pretreat the clay with appropriate surfactants [16,17]. Recently, a novel class of organic/inorganic hybrid

* Corresponding author. Tel.: 886-35727077; fax: 886-35719507.
E-mail address: kuosw@cc.nctu.edu.tw (F.C. Chang).



Scheme 1. The chemical structure and mechanism for the synthesis of benzoxazine monomers of VP-a and preparation of the benzoxazine-POSS (BZ-POSS-1) macromonomer by hydrosilylation.

materials have been developed containing the polyhedral oligomeric silsesquioxane (POSS), which contains an inorganic Si_8O_{12} core surrounded by eight hydrocarbon substituents, or seven of them plus a functional group. The POSS moiety has a unique and well-defined structure that can be used for preparing hybrid materials with well defined structures. Several reports during last few years have reported the synthesis and characterization of mono-substituted POSS derivatives. Routes to preparing nanocomposites have been developed based on a number of these derivatives, such as those bearing proton, epoxy, acrylate, or norbornyl functional group, through hydrosilylation [18], free radical [19], and ring-opening polymerizations [20].

To improve the miscibility and interactions between the inorganic Si_8O_{12} core of the POSS and the organic polybenzoxazine matrix, the POSS moiety must be attached to the polymerizable functional group of the benzoxazine unit. In this study, we synthesized a novel functionalized benzoxazine monomer containing a POSS moiety (BZ-POSS) by two different routes. One route is through the reaction of the hydro-silane-derived POSS (H-POSS) with a vinyl-terminated benzoxazine monomer (VP-a). The Si-H group can couple with the vinyl group by using a transition metal complex as a catalyst [21] such as the platinum

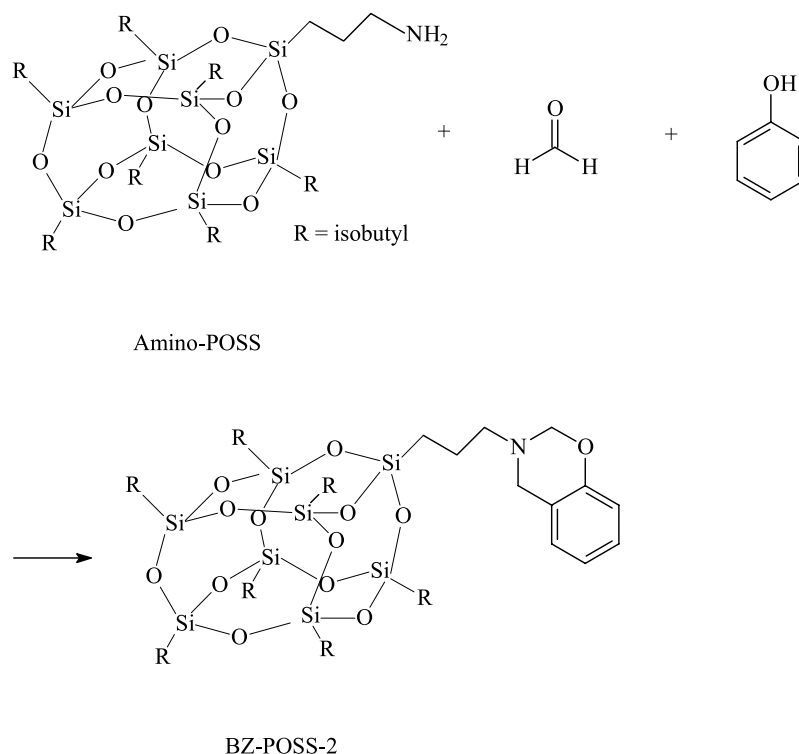
complex, Pt-dvs. The other route is by reacting a primary amine-derived POSS (Amine-POSS) with phenol and formaldehyde, which was then copolymerized with the regular benzoxazine monomer to form organic/inorganic hybrid materials possessing nano-scale silica units linked to the polymer's main chain.

These polybenzoxazine/POSS nanocomposites were prepared by a thermally induced ring-opening reaction. Thermal properties and phase morphologies of resulted nanocomposites were characterized by differential scanning calorimetry (DSC), thermal gravimetric analysis (TGA), polarized optical microscopy (POM), scanning electron microscopy (SEM) and atomic force microscopy (AFM). We found that good correlations exist between the thermal and microscopic analyses.

2. Experimental

2.1. Materials

Paraformaldehyde, phenol, allylamine, and bisphenol A were purchased from Tokyo Kasei Kogyo Co., Japan. Trichlorosilane, isobutyltrichlorosilane, and the platinum



Scheme 2. Preparation of the benzoxazine-POSS (BZ-POSS-2) macromonomer from Amine-POSS.

complex (Pt-dvs, 2 wt% Pt in xylene) were purchased from Aldrich, USA. Before use, the solution of the platinum complex was diluted 100-fold with xylene. Toluene was dried by distillation before use in the hydrosilylation reaction. Acetone, tetrahydrofuran (THF), and triethylamine (TEA) were distilled over calcium hydride before use. The POSS derivatives containing a primary amine (Amine-POSS) and a hydro-silane group (H-POSS) were purchased from the Hybrid Plastics Co., USA. The benzoxazine monomers, P-a and B-a, were purchased from Shikoku Chemicals Co., Japan.

2.2. Characterizations

^1H NMR spectra were obtained at 300 MHz using a Bruker DPX-300 Spectrometer. Infrared spectroscopic measurements were performed using a Nicolet Avatar 320 FT-IR Spectrophotometer in the range $4000\text{--}400\text{ cm}^{-1}$ at a resolution of 1.0 cm^{-1} . All sample preparations were performed under a continuous flow of nitrogen to ensure minimal oxidation or degradation of the sample. Molecular weights were determined by gel-permeation chromatography (GPC) using a SUPER CO-150 apparatus equipped with an LC gel column and an RI detector. Polystyrene samples were used as standards and THF was used as the eluent at a flow rate of 1 ml/min.

Thermal properties of the benzoxazine copolymers were characterized by DSC and TGA. DSC measurements were carried out with a DSC-910s instrument from TA Co., USA, at a scanning rate at $10\text{ }^\circ\text{C}/\text{min}$. The sample was heated at

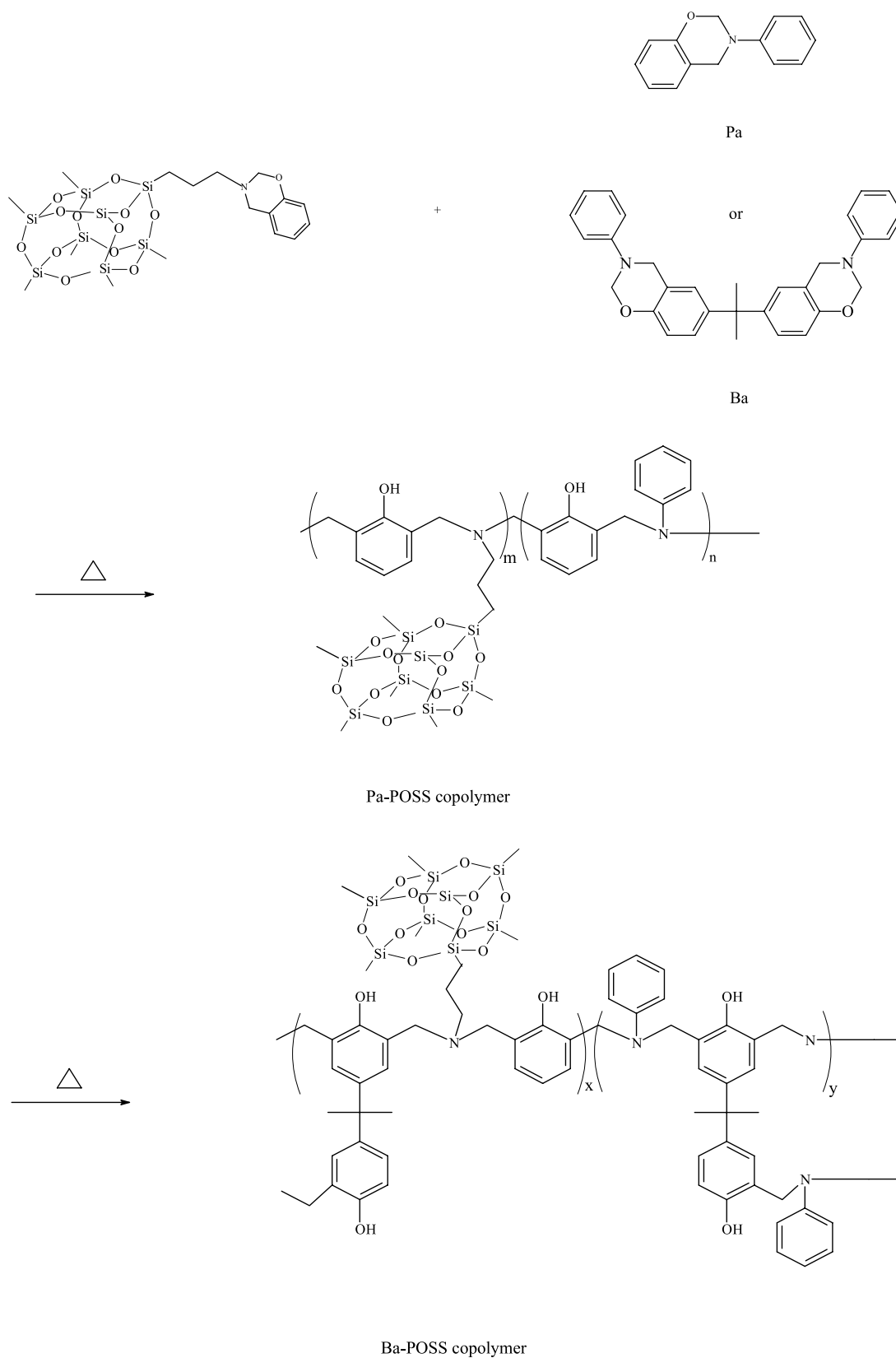
$300\text{ }^\circ\text{C}$ for 1 min and then cooled down to $30\text{ }^\circ\text{C}$ for 3 min. The sample was then reheated immediately to measure the glass transition temperature (T_g) of the copolymer. TGA was carried out using a TA Instruments TGA 2050 Thermal Gravimetric Analyzer at a heating rate of $10\text{ }^\circ\text{C}$ from room temperature to $700\text{ }^\circ\text{C}$ under a continuous flow of nitrogen.

The morphologies of BZ-POSS and its mixtures with benzoxazine were monitored before curing using an Olympus BH-651P polarized optical microscope (POM). The sample was dissolved in THF and adsorbed on a glass plate by means of spin-coating. The hybrid thin films were dried under vacuum at $40\text{ }^\circ\text{C}$ for 24 h. For analysis by AFM and SEM, these hybrids were dried under vacuum at $100\text{ }^\circ\text{C}$ for 24 h. The surface morphology was recorded using the ‘easyscan’ contact mode of an AFM system (Nanosurf AG). The spring constant of the cantilever was 5 N/m and the feedback loop bandwidth was 12 kHz. All images were recorded under an atmosphere of air at room temperature. Cross-sectional images of the polybenzoxazine/POSS nanocomposite film (0.2–0.4 mm) was investigated by SEM. The SEM image was obtained using a Hitachi-S4700I microscope operating at an acceleration voltage of 15 kV.

2.3. Syntheses

2.3.1. The vinyl-terminated benzoxazine (VP-a)

The benzoxazine monomer VP-a was prepared according to the procedure presented in Scheme 1. The synthesis and curing behavior of VP-a and its derivatives have been



Scheme 3. Preparation and chemical structures of polybenzoxazine/POSS copolymer nanocomposites.

Table 1
Properties of BZ-POSS

| POSS (theory) | M_n | M_w | M_w/M_n | C % | H % | N % |
|---------------|-----------|------------|-------------|---------------|-------------|-------------|
| BZ-POSS-1 | 968 | 1084 | 1.12 | 45.23 | 6.28 | 2.02 |
| BZ-POSS-2 | 977 (992) | 1012 (992) | 1.02 (1.00) | 47.25 (47.17) | 7.73 (7.76) | 1.48 (1.51) |

studied by Takeichi [22]. The VP-a monomer can be further purified by distillation under reduced pressure.

2.3.2. The benzoxazine-POSS (BZ-POSS-1) macromonomer

The POSS derivative bearing a benzoxazine functional group (BZ-POSS-1) was synthesized from the hydro-silane-functionalized POSS (H-POSS) and the vinyl-terminated benzoxazine (VP-a) as also depicted in Scheme 1. H-POSS (5.0 g, 6.1 mmol) and VP-a (1.4 g, 8 mmol) were dissolved in dry toluene (200 ml) and then a solution of Pt complex (Pt-dvs, 0.1 ml, 200 ppm) was injected into the solution using a syringe. The solution was then heated at 80 °C with stirring for 48 h under nitrogen. The solvent was evaporated under vacuum and the unreacted H-POSS and VP-a were extracted with warm ethanol. The resulting product, BZ-POSS-1, was obtained as a white powder (3.2 g, 53 wt% yield, mp: 55–63 °C).

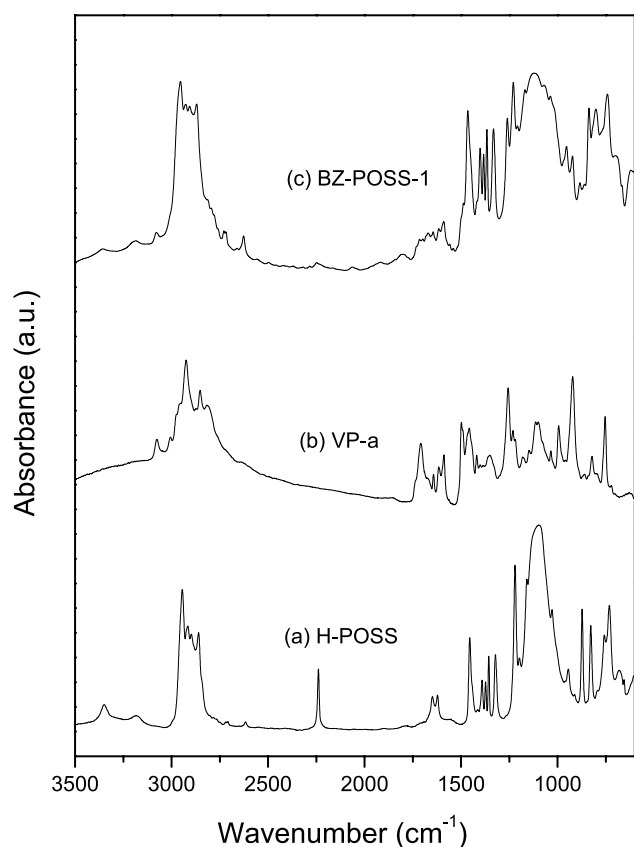


Fig. 1. IR spectra recorded at room temperature of (a) H-POSS, (b) VP-a, and (c) BZ-POSS-1.

2.3.3. The benzoxazine-POSS (BZ-POSS-2) macromonomer

BZ-POSS-2 was synthesized through procedure similar (Scheme 2) to that described above. Primary amine-functionalized POSS (Amine-POSS, 3.5 g) and phenol (0.37 g) were dissolved in THF (10 ml) in a 50-ml three-necked flask and then paraformaldehyde (0.3 g) was added at room temperature. After an additional 30 min of stirring, the temperature was raised gradually to 90 °C and the mixture was then heated under reflux for 4 h. The product was precipitated by pouring the mixture into acetonitrile (40 ml) that was stirred rapidly. The resultant product was collected by filtration and dried in a vacuum oven to yield BZ-POSS-2 as a white powder (2.2 g, 56 wt% yield, mp: 58–61 °C).

2.3.4. Preparation of hybrid copolymers of benzoxazine and POSS

P-a type benzoxazine monomer (0.95 g) and BZ-POSS-2 (0.05 g) were dissolved in THF (10 ml) and stirred for 30 min at room temperature. The solution was poured onto an aluminum plate and then left for 6 h in open air to evaporate most of the THF. The coated plate was then transferred to an oven and heated at 100 °C for 2 h. The cast film was then cured in a stepwise manner at 180 and 200 °C for 3 h each and then postcured at 220 and 240 °C for 1 h each. The cured sample was transparent and had a red-wine color with a thickness of ca. 0.2 mm. The procedure was repeated to prepare other hybrid materials by varying the amount of BZ-POSS-2 (0, 2, and 10 wt%). Finally, the hybrid material was extracted for 24 h with THF under reflux in a Soxhlet apparatus for 24 h to remove any unreacted monomers. The B-a type benzoxazine polymer and its POSS hybrid copolymers were prepared and recovered under similar conditions (Scheme 3).

3. Results and discussion

3.1. Syntheses of the benzoxazine POSS (BZ-POSS)

BZ-POSS was synthesized by two routes. Table 1 summarized results from SEC and elemental analysis (EA) for BZ-POSS-1 and BZ-POSS-2. In route one, we applied a hydrosilylation reaction using a transition metal catalyst (Pt-dvs). The mechanism involves the initial formation of a complex between the double bond of the olefin and the catalyst, which is then followed by reaction with the hydrosilane [23,24]. The successful synthesis of the

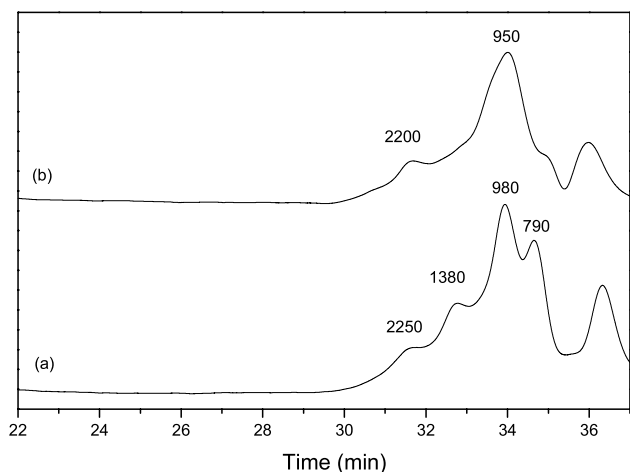


Fig. 2. Size exclusion chromatograms for (a) unpurified and (b) purified BZ-POSS-1.

BZ-POSS-1 was confirmed by its FT-IR spectrum (Fig. 1) where the Si–H stretching peak of POSS at 2200 cm^{-1} and the C=C stretching bands of the VP-a at 910 and 980 cm^{-1} are both disappeared. Other characteristic bands of the VP-a are also disappeared after hydrosilylation including the asymmetric C–O–C stretching at 1220 cm^{-1} and the stretching of its 1,2,4 substituted benzene ring at 1492 cm^{-1} . Fig. 2(a) and (b) present the SEC traces we used to determine the dispersity of molecular weights of BZ-POSS-1. In Fig. 2, SEC analysis of the synthetic BZ-POSS-1 results in a multimodal molecular weight distribution with a main peak at 980 and side peaks at 1380 and 2250 g/mol, which most likely correspond to a mixture of dimerized POSS oligomers. The hydrosilylation reaction results in a number of side reactions that have been discussed in detail previously [25–29]. The addition of the

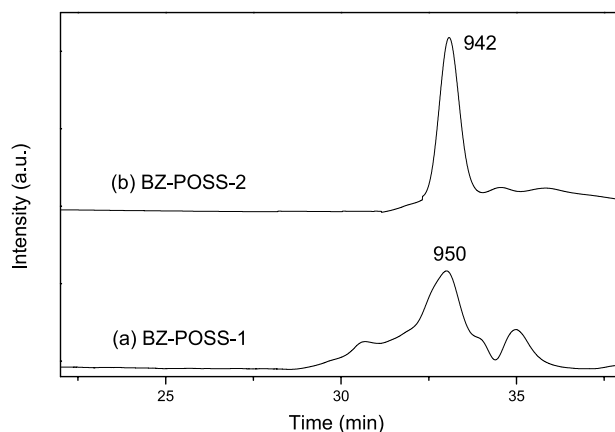


Fig. 4. Size exclusion chromatograms for (a) BZ-POSS-1 (b) BZ-POSS-2.

silane across the alkene can occur in both α and β modes, or other coupling modes. For instance, at higher-reaction temperatures, the transition metal catalyst is able to break the weak bonds of VP-a and causes a rearrangement of POSS before coupling the components together [30].

To minimize these side reactions occurring during the hydrosilylation, we investigated another method that required the POSS derivative bearing a primary amino group, Amine-POSS. This amine-POSS can react with phenol and formaldehyde without requiring any catalyst. The pure BZ-POSS-2 bearing a benzoxazine functional group can react with other benzoxazine monomers. The successful synthesis of BZ-POSS-2 was confirmed by its ^1H NMR spectrum, whose assignment is presented in Fig. 3. The resonance peaks at 6.8–7.2 ppm are assigned to the aromatic protons of BZ-POSS-2. The characteristic protons of the oxazine ring appeared at 4.81 ppm (peak g) and 3.96 ppm (peak h) assigned to $-\text{O}-\text{CH}_2-\text{N}-$ and $-\text{Ar}-\text{CH}_2-\text{N}-$, respectively. The two multiples at 2.68 ppm

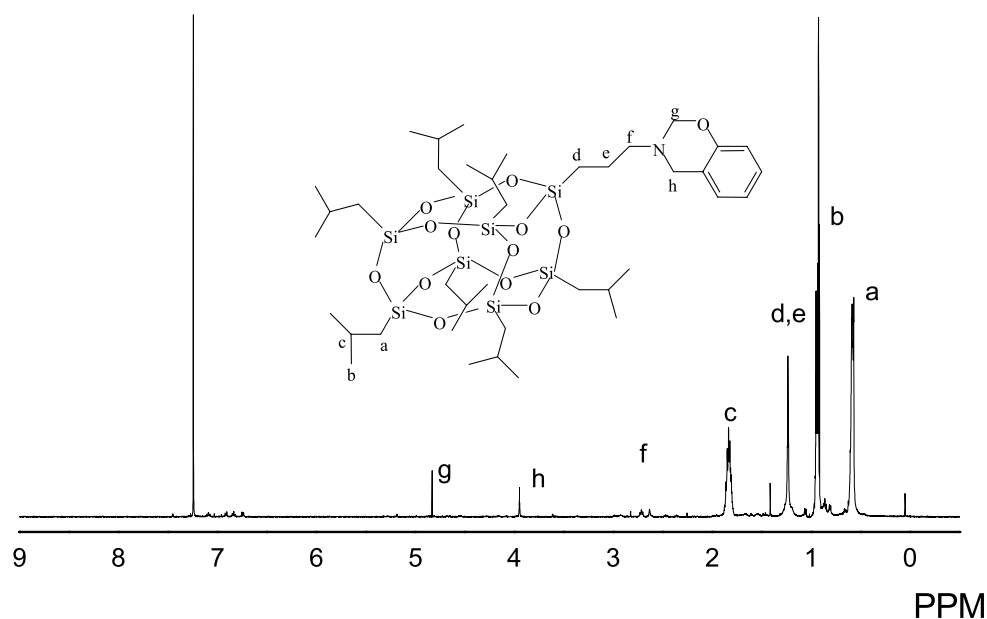


Fig. 3. ^1H NMR spectra of BZ-POSS-2.

Table 2
Summary of the thermal properties of Pa-POSS copolymer nanocomposites

| Sample | BZ-POSS-2 in feed | | T_g (°C) | 5 wt% Loss temperature (°C, in N ₂) | | Char yield in N ₂ (wt%, 800 °C) |
|--------|----------------------|-------|---------------|--|--|---|
| | wt% | mol | | | | |
| PA-0P | 0 | 0 | 138 | 308 | | 44 |
| PA-2P | 2 | 0.002 | 165 | 322 | | 46 |
| PA-5P | 5 | 0.005 | 174 | 331 | | 45 |
| PA-10P | 10 | 0.011 | 182 | 316 | | 43 |

Table 3
Summary of the thermal properties of Ba-POSS copolymer nanocomposites

| Sample | BZ-POSS-2 in feed | | T_g (°C) | 5 wt% Loss temperature (°C, in N ₂) | | Char yield in N ₂ (wt%, 800 °C) |
|--------|----------------------|-------|---------------|--|--|---|
| | wt% | mol | | | | |
| BA-0P | 0 | 0 | 162 | 310 | | 31 |
| BA-2P | 2 | 0.002 | 174 | 324 | | 48 |
| BA-5P | 5 | 0.005 | 176 | 355 | | 52 |
| BA-10P | 10 | 0.011 | 180 | 318 | | 35 |

(peak f) and 1.21 ppm (peak d and e) are typical for the protons of benzoxazine linking with POSS. The resonance peaks at 0.68 ppm (peak a), 0.93 ppm (peak b), and 1.88 ppm (peak c) are caused by the seven isobutyl hydrocarbon substituents of the POSS. NMR analysis is also consistent with the EA result (Table 1). The EA and NMR results are further substantiated by the narrow polydispersities (PDI) found from SEC analyses as shown in Fig. 4. The narrow PDI imply that dimer, trimer, or multimer products are absent through the route two.

3.2. Preparation of polybenzoxazine/POSS nanocomposites

Polybenzoxazine/POSS nanocomposite materials possess many desirable properties such as low moisture absorption, high solvent resistance, improved thermal stability, and certain desirable electronic properties. Both the benzoxazine monomer and BZ-POSS-2 are soluble in many common solvents, such as THF, toluene, chloroform, and acetone. These readily processible monomers, which can be polymerized at 200 °C that were used to synthesize hybrid copolymers having different BZ-POSS-2 contents by

ring-opening polymerization. Tables 2 and 3 summarize thermal properties of these synthesized polybenzoxazine/POSS nanocomposites. At a higher BZ-POSS-2 content (15 and 20 wt%), the prepared materials became cloudy and did not cast films under conditions similar to those used successfully at lower BZ-POSS-2 content. This result indicates that the BZ-POSS-2 macromonomer has a bulky siloxane core (ca. 1–3 nm, including side groups) that may aggregate and retard the polymerization at higher BZ-POSS-2 content.

3.3. Thermal properties of copolymer nanocomposites

The glass transition temperature of polybenzoxazine/POSS nanocomposites increases with the increase of the BZ-POSS-2 content based on Tables 2 and 3. The BZ-POSS is expected to be distributed evenly within the polymer matrix on a nanometer scale. Strong hydrogen bonding between the polymer chain and a BZ-POSS-2 nano-particle has been reported previously [31]. The interaction and miscibility between polybenzoxazine and POSS will be the subject of further study. In general, T_g of the copolymer is

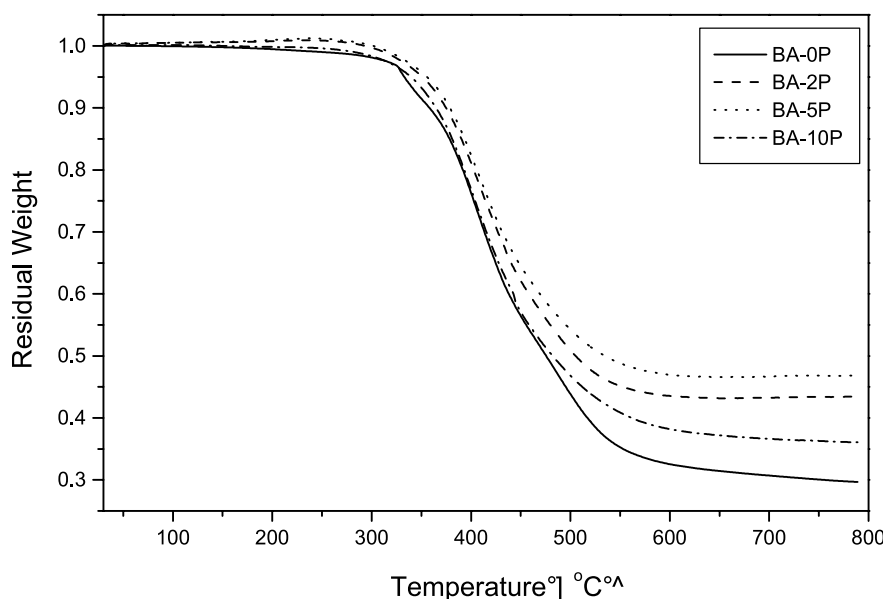
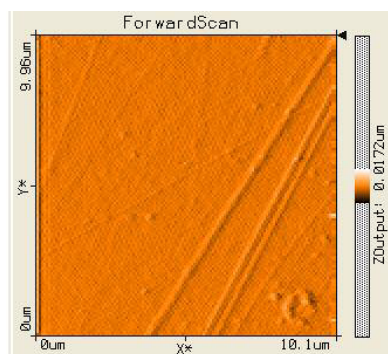
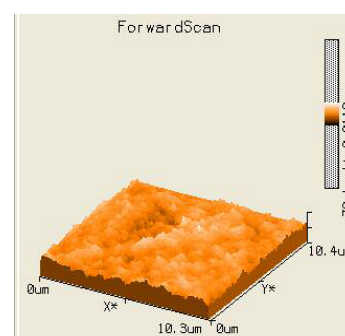
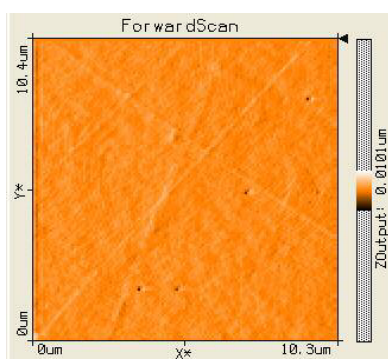


Fig. 5. TGA thermograms of B-a type polybenzoxazine having varying BZ-POSS-2 content.

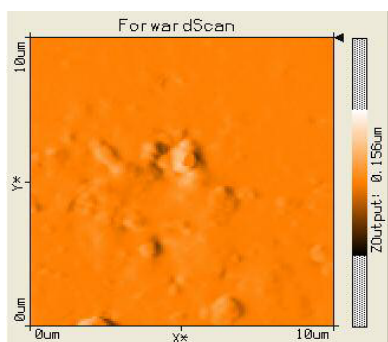
(a) Pa-0P



(b) Pa-2P



(c) Pa-5P



(d) Pa-10P

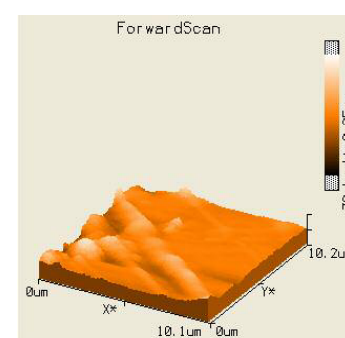
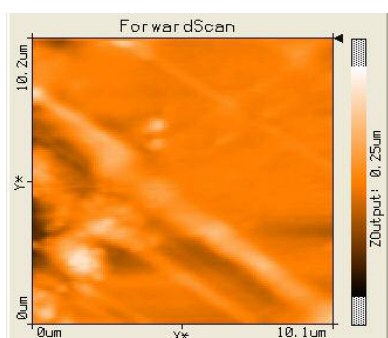


Fig. 6. AFM surface analysis of polybenzoxazine/POSS hybrid materials (a) Pure P-a type polybenzoxazine. (b) 2 wt% BZ-POSS-2 content. (c) 5 wt% BZ-POSS-2 content. (d) 10 wt% BZ-POSS-2 content. and (e) B-a type polybenzoxazine having 2 wt% BZ-POSS-2.

(e) Ba-2P

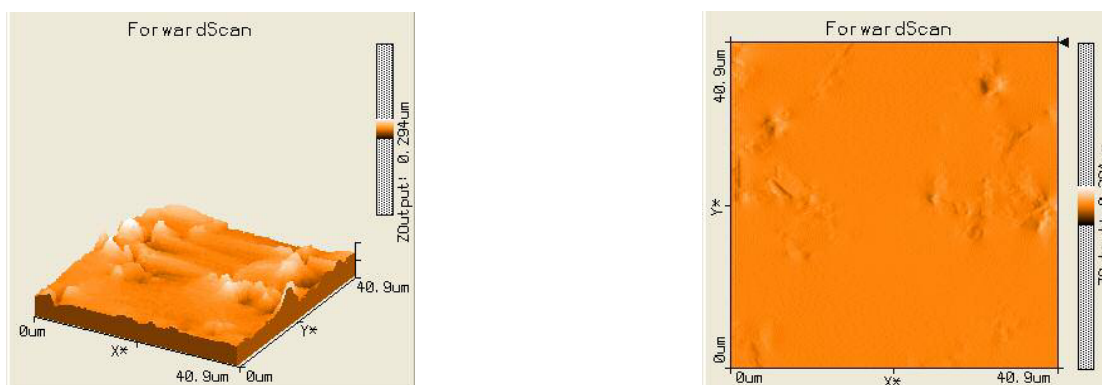


Fig. 6 (continued)

expected to be increased when these rigid BZ-POSS-2 particles are evenly dispersed on a nanometer scale within the polybenzoxazine matrix by binding the polymer chains movement.

Fig. 5 presents TGA thermograms of the polybenzoxazine/POSS nanocomposites under nitrogen atmosphere. A gradual increase in the decomposition temperature (T_d) of the Ba-POSS or Pa-POSS copolymers was observed upon increasing BZ-POSS-2 content from 0 to 5 wt%. The T_d value of the copolymer is slightly increased because of the POSS copolymer retards the movement of the molecular chains at high temperature. The aggregated BZ-POSS-2 units cause macro-phase separation when the BZ-POSS-2 content is at 10 wt%, which reduces its overall effectiveness in hindering polymer movement and its T_d value. Char yield, another indicator of thermal stability, also follows the same trend as its T_d value. The decomposition of the polybenzoxazine and the rearrangement of BZ-POSS-2 occur at higher temperatures to form a protective layer on

the surface that is probably responsible for the improved thermal stability. The hybrid with 10 wt% BZ-POSS-2 content has a lower decomposition temperature can be interpreted as the uneven distribution of the BZ-POSS-2 particles. For these polybenzoxazine/POSS hybrids, increasing the BZ-POSS-2 content leads to morphological change and, hence, microstructural analysis is useful to explain the phenomena.

3.4. Microstructural analysis

Morphologies of polybenzoxazine/POSS nanocomposites were characterized by AFM and SEM. Fig. 6 displays the AFM images of hybrids having various polybenzoxazine/POSS ratios. In Fig. 6(a) and (b), we observe that the degree of roughness of the P-a type polybenzoxazine/POSS hybrid films increases upon increasing the BZ-POSS-2 content. These nanoparticles aggregate at higher BZ-POSS-2 contents (5 and 10 wt%) more severely than the 2 wt% BZ-POSS-2 hybrid. We suggest that at higher BZ-POSS-2 content (10 wt%), the BZ-POSS-2 monomer is less miscible with benzoxazine monomer and tends to aggregate before polymerization begin. This situation can be detected by polarized optical microscopy (POM). Fig. 7 indicates that the BZ-POSS-2 aggregates are dispersed evenly (0.5–1.2 μm) in the P-a type benzoxazine matrix before curing at 10 wt% BZ-POSS-2 content. In Fig. 6(d), the AFM image of the P-a type hybrid indicates that the sizes of the nodules formed by the aggregated BZ-POSS particles are on the same dimension as those appearing before polymerization. By comparing Fig. 6(b) and (e), the domain size of the BZ-POSS-2/B-a blend is significantly greater than that of the BZ-POSS-2/P-a blend. At the same level of BZ-POSS content (2 wt%), the BZ-POSS-2/B-a blend exhibits much more gross aggregation than does the BZ-POSS-2/P-a blend. Scheme 4 presents schematic diagrams of the microstructures of the (a) P-a type and (b) B-a type polybenzoxazine/POSS hybrids. The gray background

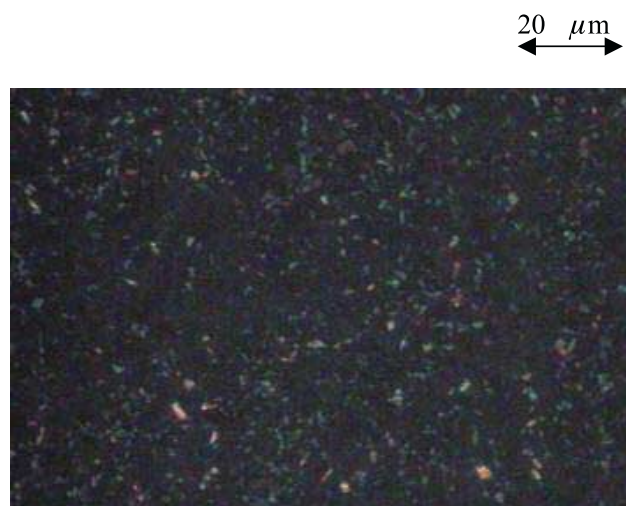
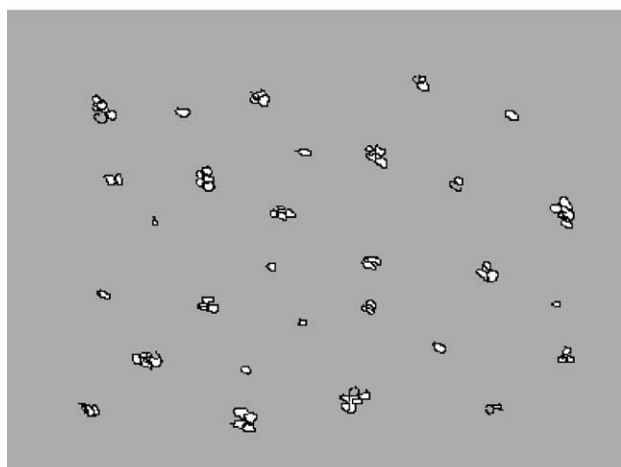
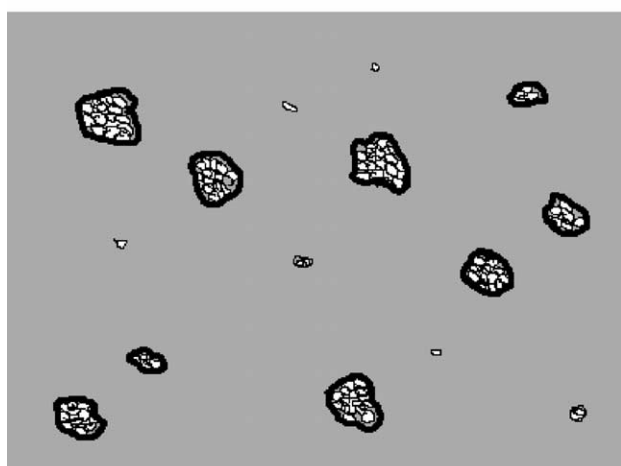


Fig. 7. POM morphology analysis of P-a type benzoxazine/POSS hybrid having 10 wt% BZ-POSS-2 content before curing.

(a)



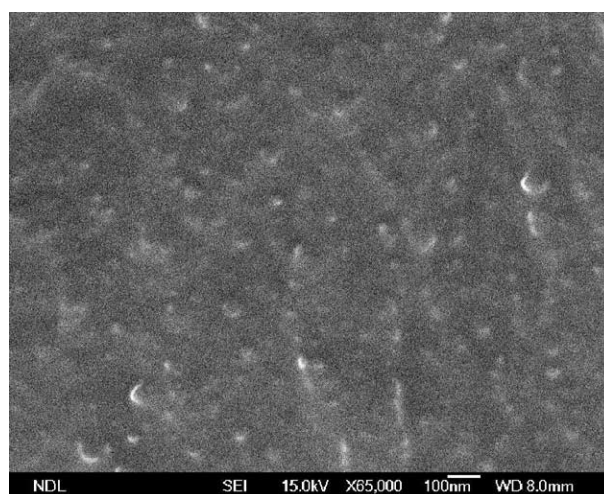
(b)



Scheme 4. Hypothetical microstructures of (a) P-a type and (b) B-a type polybenzoxazine-POSS hybrid materials.

represents the polybenzoxazine matrix and the white particles represent the BZ-POSS-2 domains. Serious aggregation of BZ-POSS-2 occurs in the B-a type polybenzoxazine matrix because of the lower miscibility of the BZ-POSS-2 monomer and the B-a type benzoxazine. When the stepwise polymerization begins, these monomer units tend to react with other monomers in their vicinity, implying that those clustered BZ-POSS-2 monomers have a greater opportunity to react with each other formed BZ-POSS-2 aggregates that are separated from the polybenzoxazine matrix. Eventually, the final product that forms is a block-like copolymer. The miscibility of the BZ-POSS-2 in the P-a type polybenzoxazine matrix is expected to be higher than that of the B-a type polybenzoxazine and, thus, the BZ-POSS-2 becomes dispersed on a nanometer scale in the P-a type polybenzoxazine at relatively lower BZ-POSS-

(a) VPa-2P



(b) VPa-5P

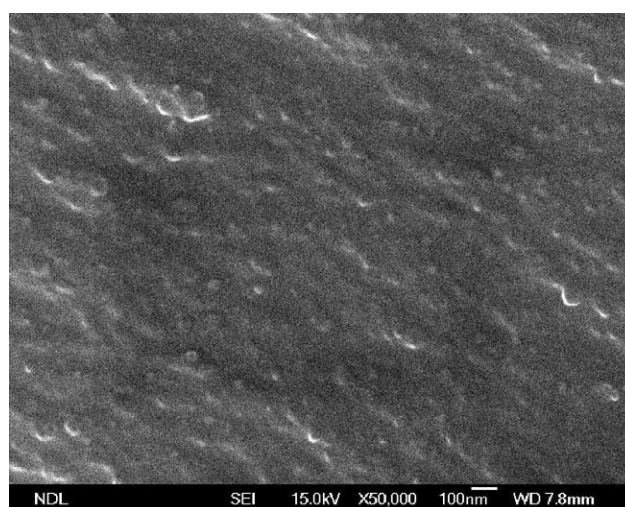


Fig. 8. SEM cross sectional analysis of polybenzoxazine/POSS hybrid material. (a) 2 wt% BZ-POSS-2 content and (b) 5 wt% BZ-POSS-2 content.

2 content. The miscibility and specific interactions between the polybenzoxazine and BZ-POSS-2 will be reported later. Fig. 8(a) and (b) display the cross sectional images obtained by SEM of materials having various BZ-POSS-2 content. The P-a type hybrid materials having BZ-POSS-2 contents of 2 and 5 wt% have almost a nano-scale distribution (20–40 nm), with the BZ-POSS-2 particles arranged evenly in the polybenzoxazine matrix.

4. Conclusions

We applied two routes to prepare BZ-POSS, one by a hydrosilylation method and another from Amine-POSS. The BZ-POSS monomer possesses a polymerizable benzoxazine

unit that is able to undergo ring-opening polymerization, which allowed a new type of polybenzoxazine-POSS nanocomposite to be prepared successfully. We prepared polybenzoxazine/POSS copolymer nanocomposites having various BZ-POSS-2 contents and examined their thermal properties by DSC and TGA. Higher BZ-POSS-2 contents resulted in the hybrid polybenzoxazine/POSS nanocomposite materials displaying apparently higher glass transition and thermal decomposition temperatures. The improvement in the thermal stability of these hybrids is less substantial, however, at higher BZ-POSS-2 content (10 wt%) as a result of gross aggregation of the BZ-POSS-2 domains.

Acknowledgements

This work was supported financially by the National Science Council, Taiwan, under contract No. NCS-92-2216-E-009-018.

References

- [1] Burke W. *J Am Chem Soc* 1954;76:1677.
- [2] Burke W. *J Org Chem* 1961;26:4403.
- [3] Burke W. *J Org Chem* 1949;71:109.
- [4] Ning X, Ishida H. *J Polym Sci, Part A: Polym Chem* 1994;32:1121.
- [5] Higginbottom, H.P. US Patent 4,501,864; 1985.
- [6] Agag T, Takeichi T. *Macromolecules* 2001;34:7257.
- [7] Kim HJ, Brunoyska ZB, Ishida H. *Polymer* 1999;40:1815.
- [8] Rimdusit S, Ishida H. *Polymer* 2000;41:7941.
- [9] Takeichi T, Guo Y, Agag T. *J Polym Sci Polym Part A: Chem* 2000;38:4165.
- [10] Takeichi T, Guo Y. *Polym J* 2001;33:437.
- [11] Su Y-C, Kuo S-W, Xu H-Y, Chang F-C. *Polymer* 2003;44:2187.
- [12] Ishida H, Allen D. *Polymer* 1996;37:4487.
- [13] Kimura H, Matsumoto A, Hasegawa K, Ohtsuka K, Fukuda A. *J Appl Polym Sci* 1998;68:1903.
- [14] Ishida H, Lee Y. *J Polym Sci Part B: Polym Phys* 2001;39:736.
- [15] Livaige J. *Bull Mater Sci* 1999;22:201.
- [16] Agag T, Takeichi T. *Polymer* 2000;41:7083.
- [17] Takeichi T, Agag T. *Polymer* 2002;43:45.
- [18] Sellinger A, Laine RM. *Macromolecules* 1996;29:2327.
- [19] Lichtenhan JD, Otonari YA, Carr MJ. *Macromolecules* 1995;28:8435.
- [20] Zheng L, Farris RJ. *J Polym Sci, Polym Chem Ed* 2001;39:2920.
- [21] Ojima I. In: Patai S, Rappoport S, editors. *The chemistry of organic silicon compounds*. New York: Wiley; 1989.
- [22] Takeichi T, Agag T. *Macromolecules* 2003;36:6010.
- [23] Burke WJ. *J Am Chem Soc* 1949;71:609.
- [24] Chalk AJ, Harrod JF. *J Am Chem Soc* 1965;87:16.
- [25] Chalk AJ, Harrod JF. *J Am Chem Soc* 1965;87:1183.
- [26] Belyakova ZC, Golubtsova SA, Yakusheva TM. *Russ J Gen Chem* 1965;35:1187.
- [27] Muslof MC, Speier JL. *J Org Chem* 1964;29:2519.
- [28] Takeuchi R, Yasue H. *Organometallics* 1996;15:2098.
- [29] Tanke RS, Crabtree RH. *Organometallics* 1991;10:415.
- [30] Lapointe AM, Rix FC, Brookhart M. *J Am Chem Soc* 1997;119:906.
- [31] Akhren IS, Chistovalova NM, Volpin ME. *Russ Chem Rev* 1983;52:542.